Int. J. Electrochem. Sci., 12 **(2017)** 6930 – 6939, doi: 10.20964/2017.08.13

International Journal of
ELECTROCHEMICAL
SCIENCE
www.electrochemsci.org

Enhanced Electrochemical Performance of $LiFePO_4$ as Cathode for Lithium Ion Battery by Codoping with Titanium and Nitrogen

Wei Su[1], *Kaiqi Xu*[1,2,*], *Guobin Zhong*[1], *Zengfu Wei*[1], *Chao Wang*[1], *Yuezhong Meng*[2,*]

[1] Electric Power Research Institute of Guangdong Power Grid Co., Ltd., Guangzhou 510080, China
[2] State Key Laboratory of Optoelectronic Materials and Technologies/ The Key Laboratory of Low-carbon Chemistry & Energy Conservation of Guangdong Province, Sun Yat-sen University, Guangzhou 510275, P. R. China
[*]E-mail: xukaiqi@yeah.net, mengyzh@mail.sysu.edu.cn

Received: 21 April 2017 / *Accepted:* 29 May 2017 / *Published:* 12 July 2017

Titanium and nitrogen codoped $LiFePO_4$ was synthesized via a simple solid state reaction using TiN as the dopant source. The morphology, structure, valence state and electrochemical performance of all the samples were investigated and compared with the undoped $LiFePO_4$. The results showed that the codoped samples maintained an olivine structure with modified lattice parameters and exhibited a prominent improved electrochemical performance. Among all the codoped samples, $LiFe_{0.94}Ti_{0.04}PO_{4-\sigma}N_{0.04}$ showed the best rate capability of 108.1 mAh g^{-1} even at a high rate of 5 C and exhibited a capacity retention of about 94% after 100 cycles at 1 C.

Keywords: Lithium ion batteries; Cathode; $LiFePO_4$; Codoping

1. INTRODUCTION

The olivine $LiFePO_4$ was first reported by Goodenough in 1997 [1]. $LiFePO_4$ comprised of earth-abundant and non-toxic elements is highly safe and also with long cycle life. Because of these advantages, it has been recognized as a promising cathode for lithium ion battery using in the field of electric vehicle and energy storage. However, the poor intrinsic electronic and ionic conductivity hampered its extensive application until Armand set up a synthesis leading directly to carbon coated particles [2,3]. Carbon coating is the most effective method to improve the electronic conductivity of the $LiFePO_4$. With carbon coating, $LiFePO_4$ exhibits a capacity close to the theoretical capacity of 170 mAh g^{-1} [3]. In addition, reducing particle size can also make prominent improved electrochemical

performance resulting from the shorten diffusion length for electrons and lithium ions [4]. Nowadays, carbon coating and nanocrystallizition have been the most widely used methods to improve the performance of $LiFePO_4$.

In spite of its commercial success, there are still challenges for future energy storage of $LiFePO_4$ [5]. Carbon coating can enhance the apparent conductivity of the $LiFePO_4$/C composite but it can't change the intrinsic conductivity of the $LiFePO_4$. In contrast to the methods mentioned above, doping heterogeneous elements is reported to be an efficient way to enhance the intrinsic conductivity. Chung firstly reported that doping with supervalent cations (Nb^{5+}, Ti^{4+}, Zr^{4+}, Al^{3+}, Mg^{2+}) at Li site in $LiFePO_4$ could increase the electronic conductivity by 8 orders of magnitude [6]. But up to now, aliovalent doping at Li site is still controversial [7-11]. First-principle calculation and experiment show that metal cations doping at Fe site can improve the conductivity and electrochemical performance of $LiFePO_4$ [12-14]. In addition to the cationic substitution, anionic doping is also effective, such as doping with, Cl^- and F^- [15,16]. Compared with the cationic or anionic doping, codoping has received less attention. The electrochemical performance of $LiFePO_4$ is expected to be further enhanced by the synergistic effect of cation and anion codoping [17].

In this work, Ti and N codoped $LiFePO_4$ was synthesized via a simple solid state reaction using TiN as the dopant source. The morphology, structure, valence state and electrochemical performance of all the samples were investigated and compared with the undoped $LiFePO_4$.

2. EXPERIMENTAL

2.1 Materials synthesis

Undoped and codoped $LiFePO_4$ was synthesized using a two-step solid-state reaction. Li_2CO_3 (99%), $FeC_2O_4{\cdot}2H_2O$ (99%), $NH_4H_2PO_4$ (99.5%) from Aldrich were used as the raw materials for the synthesis of $LiFePO_4$ without further treatment. TiN (99%) from Aladdin was employed to dope the $LiFePO_4$. For the undoped $LiFePO_4$, stoichiometric amounts of starting materials were mixed with ethanol and milled for 6 h using a zirconia milling media. Subsequently, the mixture was dried and ground in an argon environment. Then the fine powder was calcined in Ar/H_2 (95:5 v/v) at 350 °C for 5 h. The intermediate product was ground again after cooling to room temperature, and then calcined at 600 °C for 8 h. The codoped samples ($LiFe_{1-3x/2}Ti_xPO_{4-\sigma}N_x$, x = 0.02, 0.04 and 0.06) were similarly prepared by grinding the intermediate product with stoichiometric amounts of TiN.

2.2 Material characterization

Scanning electron microscope (SEM, Hitachi S-4800), Energy Dispersive X-ray mapping (EDX) was utilized to examine the morphology and elemental distribution. A Bruker D8 Advance X-ray diffractometer (XRD) with Cu Kα radiation (λ=1.5418 Å) was used to analyze the phase compositions. The chemical states of Ti and N were identified using X-ray photoelectron spectroscopy (XPS, ESCALAB250Xi, Thermo, USA). The binding energy was calibrated with C1s (284.8 eV) of

contaminated carbon in the vacuum chamber. The molar ratios of Li, Fe, P and Ti were obtained by inductively coupled plasma atomic emission spectroscopy (ICP-AES) while the concentration of N was obtained by nitrogen/oxygen determinator. Electrochemical impedance spectroscopy (EIS) was performed on an impedance analyzer (IM6ex) with 5 mV AC signals ranging from 100 mHz to 1MHz by using coin cell.

2.3 Electrochemical measurements

Electrochemical performances were tested in CR2032-type coin cells. The working electrodes contained active material, carbon black and polyvinylidene fluoride in a weight ratio of 8: 1: 1. In order to further enhance the electrical conductivity of the active material, the intermediate product was ground with 2 wt.% carbon black or equal amounts of polyacrylonitrile before calcined. Lithium foil was used as the counter electrode. The electrolyte was 1 M $LiPF_6$ dissolved in ethylene carbonate (EC): dimethyl carbonate (DMC) (1: 1 v/v). The cell was cycled between 2.5 and 4.2 V vs. Li/Li^+. The current density for 1C rate performance was 150 mA g^{-1}.

3. RESULTS AND DISCUSSION

Supervalent cation is designed to dope into the lattice of $LiFePO_4$ to replace Fe^{2+} while O^{2-} is substituted by N^{3-} to make atomic vacancies and keep charge balance. Owing to the change of the crystal structure and the atomic vacancies, the conductivity of $LiFePO_4$ may get improved. Various compounds can provide supervalent cation while the source of N^{3-} is limited. Li_3N can provide both Li^+ and N^{3-}, but Li_3N suffers rapid hydrolysis in air. NH_3 is not safe and difficult to operate. Based on these factors, TiN is chosen as the dopant source for its high stability. **Table 1** lists the molar ratios of elements for the samples with different Ti and N codoping amounts. The undoped $LiFePO_4$ is named as LFP, and the codoped samples ($LiFe_{1-3x/2}Ti_xPO_{4-\sigma}N_x$, x = 0.02, 0.04 and 0.06) are named as TN002, TN004 and TN006, respectively. It is found that the experimental molar ratios are very close to the theoretical values. After calcined at high temperature, most of the elements are retained and only a few nitrogen loss.

Table 1. Theoretical and experimental molar ratios of elements for $LiFe_{1-3x/2}Ti_xPO_{4-\sigma}N_x$.

	Samples	Li	Fe	P	Ti	N
Theoretical	LFP	1.000	1.000	1.000	-	-
	TN002	1.000	0.970	1.000	0.020	0.020
	TN004	1.000	0.940	1.000	0.040	0.040
	TN006	1.000	0.910	1.000	0.060	0.060
Experimental	LFP	0.999	0.994	1.000	-	-
	TN002	1.008	0.969	1.000	0.018	0.010
	TN004	1.006	0.938	1.000	0.036	0.030
	TN006	0.994	0.915	1.000	0.053	0.044

Fig.1 shows the SEM images and EDX mapping images of the as-obtained undoped $LiFePO_4$ and the codoped $LiFePO_4$. The nanoparticles are distributed uniformly and have a typical diameter of about 50 nm with near-spherical shape. It suggests that Ti and N codoping doesn't change the morphology of the particle. This result is somewhat different from the previous literature, in which the average particle size of the Ti doped $LiFePO_4$ was slightly increased [18]. This may be attributed to N atoms. EDX mapping was utilized to examine the elemental distribution of the codoped sample as shown in **Fig. 1e**. P, Ti and Fe are homogeneously dispersed in the sample. It is indicated that the doping element Ti may have distributed in every individual particle. As we know, X-ray detector used in the EDX system is usually not sensitive to light elements. Therefore, no obvious signal of Li and N is present in the EDX spectrum. The concentration of N was obtained by nitrogen/oxygen determinator and would be further analyzed by XPS below.

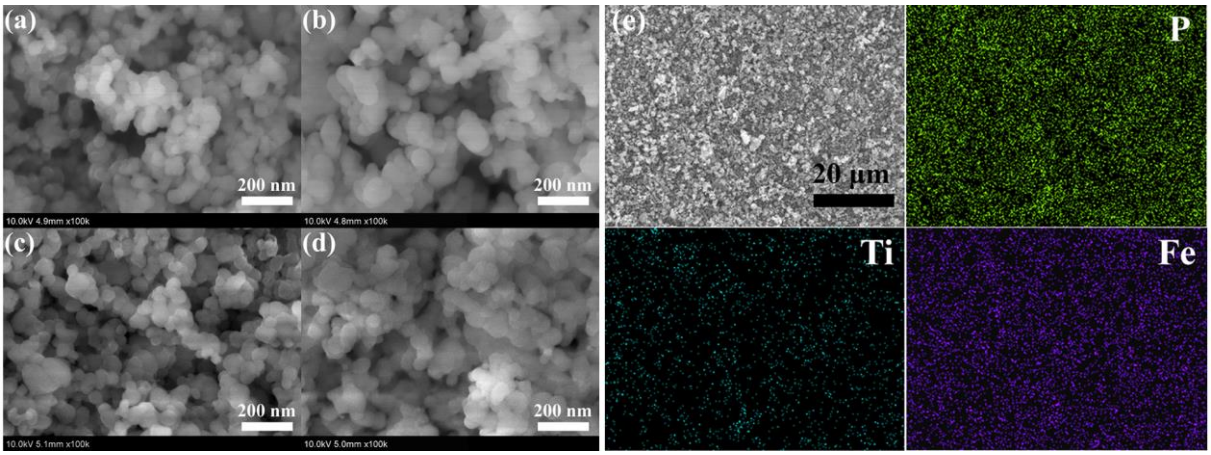

Figure 1. SEM images of the undoped $LiFePO_4$ (a) LFP, and the codoped $LiFePO_4$ (b) TN002, (c) TN004, (d) TN006, and (e) EDX mapping images of the codoped $LiFePO_4$.

Fig. 2 shows the typical powder XRD pattern of the undoped $LiFePO_4$ and the codoped $LiFePO_4$. The observed XRD patterns of all samples are well in accordance with the standard olivine-type $LiFePO_4$ with orthorhombic crystal structure (JCPDS No.81-1173). No extra diffraction peak is observed for the codoped $LiFePO_4$. It indicates that Ti and N probably enter into the lattice of $LiFePO_4$ rather than forming impurities. The substitution of Ti and N in Fe and O sites doesn't affect the formation of a single phase and this is probably due to the concentration of both Ti and N are too low to induce the structural change. When the doping concentration of Ti increases to a certain extent (e.g. 8 at.%), impurities such as $Li_3Fe_2(PO_4)_3$ and $Li_2TiFe(PO_4)_3$ would be formed [18]. Therefore, doping concentration was limited to 6 at.% in this work. TiN can react with H_2O at high temperature leading to the loss of nitrogen. Therefore, the $LiFe_{1-3x/2}Ti_xPO_{4-\sigma}N_x$ was synthesized via a two-step solid-state reaction. The H_2O generated in the solid-state reaction was eliminated at the pre-sintering step. Specifically, the raw materials was firstly calcined at 350 °C for 5 hours to obtain the pre-sintering product, which was then ground with stoichiometric amounts of TiN following by a calcination at 600 °C for 8 h. The adherence between TiN and $LiFePO_4$ is proved excellent and the diffusion of Ti into

$LiFePO_4$ is found to be easy at high temperature [19]. Moreover, the particle size of TiN is only 20 nm that would be highly reactive. In order to confirm that the TiN has reacted with the intermediate product, XRD patterns of TiN, the intermediate mixture and the codoped sample TN006 are carefully compared as shown in **Fig. 2e-2g**. The (200) diffraction peak of TiN is observed for the intermediate mixture (**Fig. 2e, 2g**), but this characteristic peak disappears after calcination at 600 °C (**Fig. 2f**). TiN is involved in the solid-state reaction and no impurity is formed. It suggests that Ti and N probably enter into the crystal lattices of $LiFePO_4$.

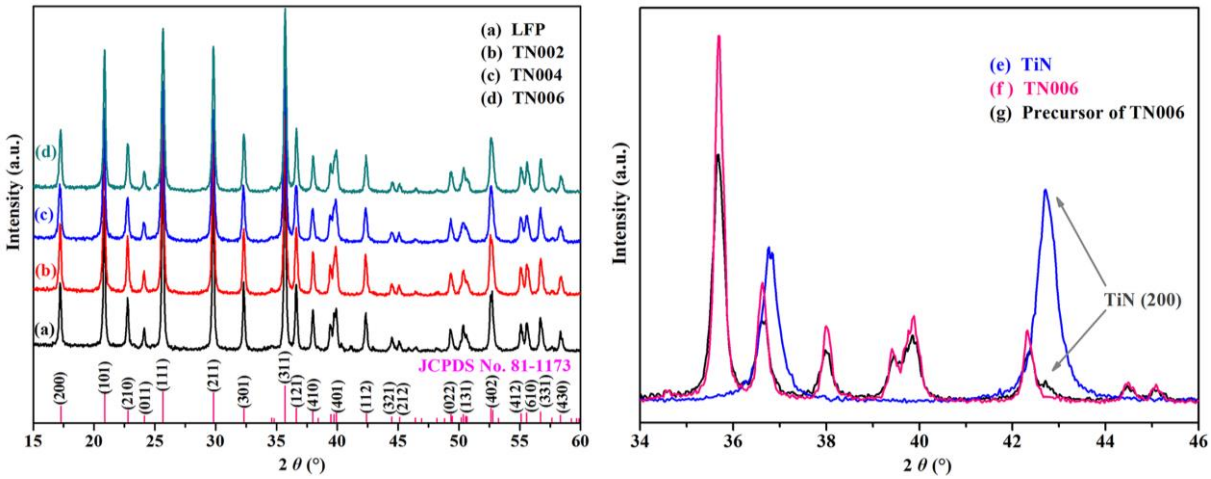

Figure 2. XRD patterns of (a) the undoped $LiFePO_4$ LFP, the codoped $LiFePO_4$ (b) TN002, (c) TN004, (d) TN006, (e) pristine TiN, (f) TN006, and (g) the precursor of TN006.

According to the literature, Ti^{4+} cation is preferred to replace the Fe sites in the olivine $LiFePO_4$ structure and substitution of N for O is also theoretically feasible on the basis of the first-principles calculations [20,21]. In the previous works, Ti^{4+} was doped at Fe^{2+} site by two methods. One is replacing Fe^{2+} with equal molar ratio of Ti^{4+} to form $LiFe_{1-x}Ti_xPO_4$ and the other is replacing Fe^{2+} with equal valence of Ti^{4+} to form $LiFe_{1-2x}Ti_xPO_4$. For the former, impurities such as Li_3PO_4 would be formed even the doping concentration was limited to 1 at.% [22]. In spite of the impurities, $LiFe_{1-x}Ti_xPO_4$ shows improved electrochemical performance. For the $LiFe_{1-2x}Ti_xPO_4$, it shows smaller energy gap and higher electronic conductivity [23]. As to the N doping, first-principles calculations show that the substitution of N for O on the (010) surface of the $LiFePO_4$ is energetically favored and significantly decreases the band gap of the $LiFePO_4$, resulting in better electronic conductivity and faster Li^+ transport [24]. The electrochemical performance of Ti and N codoped $LiFePO_4$ is expected to be further enhanced by the synergistic effect. But the structure of this codoped $LiFePO_4$ has never been studied. In order to confirm the doping result and clarify the change of the crystal structure, XRD patterns of all samples were further analyzed by Rietveld refinements. The corresponding structural parameters are listed in **Table 2**. The reliability factors Rwp of the refinement are less than 10%, demonstrating that the results are reliable and the codoped samples are all single-phase with no any impurities. Compared with the standard olivine-type $LiFePO_4$ (a = 10.332 Å, b = 6.010 Å, c = 4.692 Å and V = 291.35 $Å^3$), the unit cell volumes of the codoped samples shrink and the lattice parameters also decrease slightly. Volumetric shrinkage is caused by that the radius of $Ti^{3+/4+}$ is smaller than that

of Fe^{2+} and the formation of Fe-vacancy and O-vacancy, but the radius of O^{2-} and N^{3-} is similar [25]. This result is consistent with previous literatures [23,26-29]. The changed lattice constants and credible reliability factor of the refinement indicate that the Ti and N ions have been successfully doped into the $LiFePO_4$ phase.

Table 2. Lattice parameters of $LiFe_{1-3x/2}Ti_xPO_{4-\sigma}N_x$

	a(Å)	*b*(Å)	*c*(Å)	*V*(Å^3)	Rp	Rwp
LFP	10.3220	6.0046	4.6909	290.740	8.45	10.40
TN002	10.3196	6.0036	4.6916	290.667	7.78	8.45
TN004	10.3189	6.0040	4.6914	290.654	6.85	7.88
TN006	10.3144	6.0031	4.6916	290.496	7.16	8.27

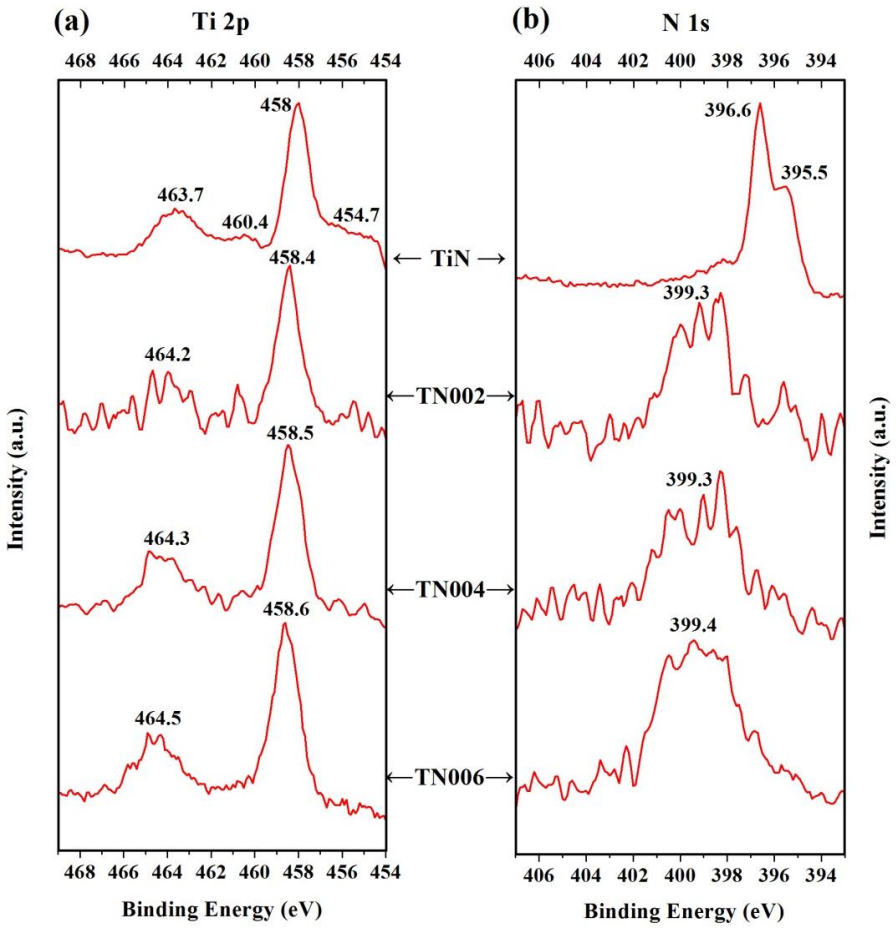

Figure 3. XPS spectrum of the TiN and the codoped $LiFePO_4$, (a) Ti-2*p* spectrum, (b) N-1*s* spectrum.

The chemical states of Ti and N were identified using XPS as shown in **Fig. 3**. The binding energy was calibrated with C1s (284.8 eV) of contaminated carbon in the vacuum chamber. The Ti-2*p* spectrum exhibits two contributions, $2p_{1/2}$ and $2p_{3/2}$, resulting from the spin–orbit splitting. In **Fig. 3a**, the Ti-2*p* spectrum for the raw material TiN shows four peaks which are attributed to amorphous TiO_2 (Ti-$2p_{1/2}$: 463.7 eV, Ti-$2p_{3/2}$: 458.0 eV) and TiN (Ti-$2p_{1/2}$: 460.4 eV, Ti-$2p_{3/2}$: 454.7 eV) [30,31]. Nano TiN is easily oxidized in the air and forms a surface oxide layer. According to the literature, Ti^{3+} could easily transform to Ti^{4+} at high temperature, which is in agreement with our work that the Ti-2*p* peaks for the codoped samples are attributed to Ti^{4+} [30]. Compared to the surface oxide on TiN, the binding energy of Ti^{4+} in $LiFe_{1-3x/2}Ti_xPO_{4-\sigma}N_x$ is about 0.5 eV higher. It is probably due to the change of the environment that around Ti atoms which are doped into the crystal structure of $LiFePO_4$. The N-1*s* spectrum for the TiN exhibits two peaks. The 396.6 eV can be attributed to TiN and the 395.5 eV may be attributed to titanium oxynitride (**Fig. 3b**). For the codoped samples, the N-1*s* peak shifts to a higher binding energy (399.3 eV) resulting from the newly formed P-N bonds which is similar with LiPON [32,33]. The XPS results indicate that N atoms are also doped into $LiFePO_4$.

Fig. 4 displays the charge and discharge curves, the rate performance and the cycling performance of the $LiFe_{1-3x/2}Ti_xPO_{4-\sigma}N_x$. Each of the charge/discharge curves consists of a charge voltage plateau and a corresponding discharge voltage plateau at near 3.4 V, which is the result of a two-phase reaction based on the redox couple of Fe^{2+}/Fe^{3+} during Li^+ extraction and insertion process. The specific capacities of the codoped samples firstly increase with a codoping concentration of 2 at% and then decrease until the codoping amount up to 6 at% when cycled at 0.1 C. Specifically, the initial capacity is 146.5 mAh g^{-1}, 150.3 mAh g^{-1}, 148.2 mAh g^{-1} and 145.8 mAh g^{-1} for LFP, TN002, TN004 and TN006, respectively. The capacity of $LiFePO_4$ is improved by codoping appropriate amount of Ti and N. It has been suggested in literatures that the increased electrical conductivity induced by the heterogeneous ion doping has attributed to the improved electrochemical performance [6,11]. But excessive Ti will reduce the relative ratio of the Fe, and consequently lead to a decrease in capacity. In order to evaluate the rate performance of $LiFe_{1-3x/2}Ti_xPO_{4-\sigma}N_x$, the cells were cycled at different rates from 0.1 C to 5 C. It is found that the codoping samples exhibit a lower polarization and show better rate capability than $LiFePO_4$, especially the high rate capability. All the samples deliver approximate capacities at the rate below 0.5 C, but the difference of the capacity grows ever greater as the rate increases. The codoping samples deliver much higher capacities. TN004 displays the best rate capability among all the samples. The capacity degradation and voltage drop of TN004 are minimum when the discharging rate is increased from 0.1 C to 5 C. TN004 delivers discharge capacities of 148.2 (0.1 C), 136.1 (0.5 C), 134.1 (1 C), 119.6 (2 C), and 108.1 mAh g^{-1} (5 C), respectively. On the contrast, LFP delivers less discharge capacity which are 146.5 (0.1 C), 137.6 (0.5 C), 126.8 (1 C), 101.0 (2 C), and 82.5 mAh g^{-1} (5 C), respectively. Cycling performances of all the samples are shown in **Fig. 4e**. LFP possesses a capacity retention of 93% after 100 cycles at 1 C and TN002 delivers the highest capacity retention of 94.1%. The cycling performance of TN006 becomes a little worse. This may result from the instability of the crystal structure caused by the high defect concentration. Nevertheless, the rate performance and the cycling performance are evidently improved with proper codoping concentration of Ti and N.

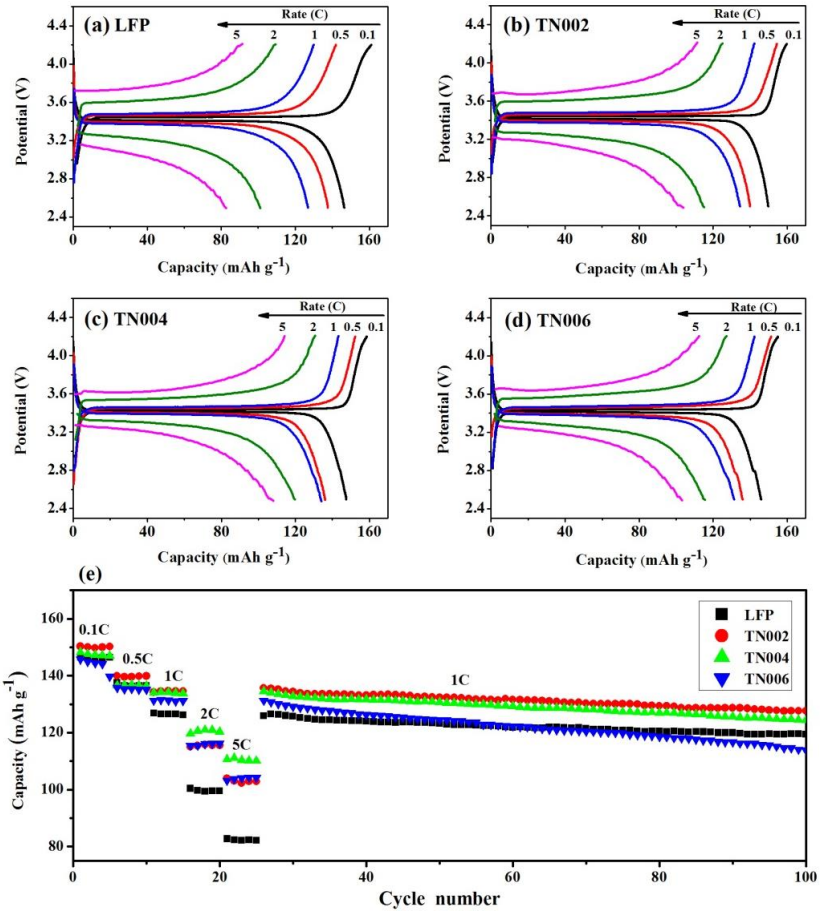

Figure 4. Charge and discharge curves of $LiFe_{1-3x/2}Ti_xPO_{4-\sigma}N_x$, (a) LFP, (b) TN002, (c) TN004, (d) TN006, and (e) the rate performance and the cycling performance. The cell was cycled between 2.5 and 4.2 V *vs.* Li/Li^+.

Ti doping or N doping can reduce the charge transfer resistance [25-29,33,34]. Herein, the lithium ion insertion and deinsertion kinetics of $LiFe_{1-3x/2}Ti_xPO_{4-\sigma}N_x$ were investigated by the electrochemical impedance. Nyquist plots for undoped and codoped samples are presented in **Fig. 5**. It can be seen that all profiles exhibit one semicircle in the high frequency region and a straight line in the low frequency region. The semicircle is related to the charge transfer process of the electrochemical reaction. The inclined line at the low frequency region corresponds to the lithium ion diffusion process within the cathode material which is called Warburg impedance [35]. The charge transfer resistance of pristine LFP, TN002, TN004 and TN006 are about 160 Ω, 120 Ω, 128 Ω and 140 Ω, respectively. A significant decrease of charge transfer resistance is observed for the codoped samples in the high frequency region, revealing that the Ti and N codoping greatly facilitates the kinetic process during charge/discharge and leads to the improvement of the electrochemical performance. Also, the electrical conductivity of the $LiFe_{1-3x/2}Ti_xPO_{4-\sigma}N_x$ with identical carbon content was measured by linear voltammetry. The electrical conductivity of the LFP, TN002, TN004 and TN006 are about 3.7×10^{-5} S cm^{-1}, 5.1×10^{-4} S cm^{-1}, 4.6×10^{-4} S cm^{-1} and 2.9×10^{-4} S cm^{-1}, respectively. The electrical conductivities of the codoped samples are improved significantly. Generally, low Warburg impedance indicates faster lithium ion diffusion. It can be found that the Warburg impedance

of the codoped sample is smaller than that of pristine LFP. The obtained results reveal that codoping provides a more excellent kinetic behavior, which is consistent with the cycling and rate performance.

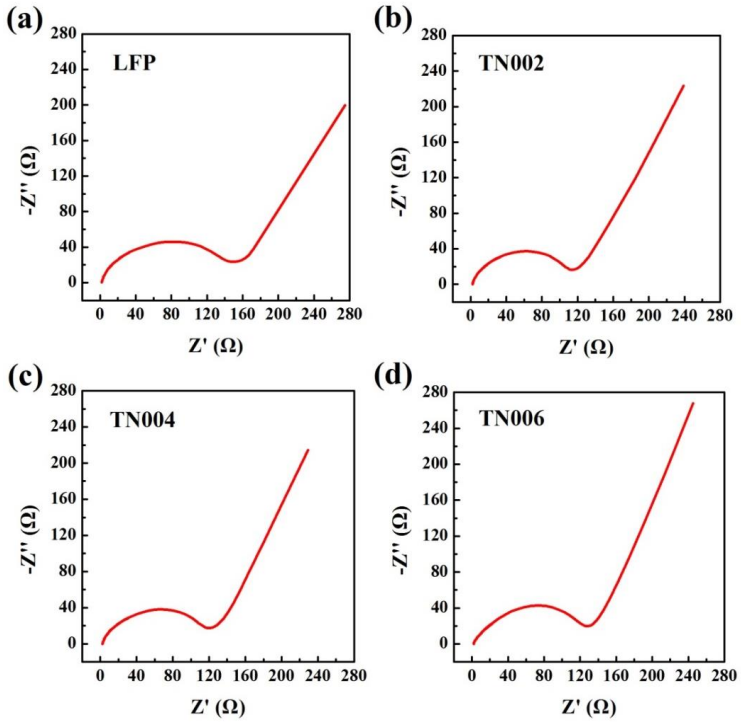

Figure 5. The electrochemical impedance spectra of the undoped $LiFePO_4$ (a) LFP, and the codoped $LiFePO_4$ (b) TN002, (c) TN004, and (d) TN006.

4. CONCLUSIONS

In summary, Ti and N codoped $LiFe_{1-3x/2}Ti_xPO_{4-\sigma}N_x$, (x = 0.02, 0.04 and 0.06) cathode materials are successfully synthesized by a simple solid-state method using TiN as dopant source. Ti and N entering into the lattice of $LiFePO_4$ doesn't alter the particle morphology and the orthorhombic structure but slightly changes the lattice parameters. Rietveld refinements and XPS evidently confirm that the Ti and N ions are successfully introduced into the crystal lattice of $LiFePO_4$. The codoped samples exhibit better electrochemical performance compared to the undoped $LiFePO_4$, especially for high rate performance. Among all the codoped samples, $LiFe_{0.94}Ti_{0.04}PO_{4-\sigma}N_{0.04}$ showed the best rate capability of 108.1 mAh g^{-1} even at a high rate of 5 C and exhibited a capacity retention of about 94% after 100 cycles at 1 C. Therefore, Ti and N codoping is an effective way to attain high performance phosphate positive materials.

ACKNOWLEDGEMENTS
This work was supported by the China Southern Power Grid Co., Ltd. (Grant No. GDKJXM00000039 and Grant No. GDKJXM20161890).

References

1. A. K. Padhi, J. B. Goodenough, and K. S. Nanjundaswamy, *J. Electrochem. Soc.*, 144 (1997) 1188.
2. N. Ravet, J. B. Goodenough, S. Besner, M. Simoneau, P. Hovington and M. Armand, 196th Electrochemical Society Meeting, Honolulu, Hawaii, USA, Oct 1999, Extended Abstract no 127.
3. N. Ravet, Y. Chouinard, and M. Armand, *J. Power Sources*, 97 (2001) 503.
4. A. Yamada, S. C. Chung and K. Hinokuma, *J. Electrochem. Soc.*, 148 (2001) A224.
5. J. J. Wang and X. L. Sun, *Energy Environ. Sci.*, 8 (2015) 1110.
6. S. Y. Chung, J. T. Bloking and Y. M. Chiang, *Nat. Mater.*, 1 (2002) 123.
7. P. S. Herle, B. Ellis, N. Coombs and L. F. Nazar, *Nat. Mater.*, 3 (2004) 147.
8. Y. H. Rho, L. F. Nazar, L. Perry and D. Ryan, *J. Electrochem. Soc.*, 154 (2007) A283.
9. M. Wagemaker, B. L. Ellis, D. Luetzenkirchen-Hecht, F. M. Mulder and L. F. Nazar, *Chem. Mater.*, 20 (2008) 6313.
10. K. Zaghib, A. Mauger, J. B. Goodenough, F. Gendron and C. M. Julien, *Chem. Mater.*, 19 (2007) 3740.
11. S. Q. Shi, L. J. Liu, C. Y. Ouyang, D. S. Wang, Z. X. Wang, L. Q. Chen and X. J. Huang, *Phys, Rev. B*, 68 (2003) 195108
12. F. Omenya, N. A. Chernova, S. Upreti, P. Y. Zavalij, K. W. Nam, X. Q. Yang and M. S. Whittingham, *Chem. Mater.*, 23 (2011) 4733.
13. D. Y. Wang, H. Li, S. S. Shi, X. J. Huang and L. Q. Chen, *Electrochim. Acta*, 50 (2005) 2955.
14. F. Omenya, N. A. Chernova, R. Zhang, and M. S. Whittingham, *Chem. Mater.*, 25 (2013) 85.
15. C. S. Sun, Y. Zhang, X. J. Zhang and Z. Zhou, *J. Power Sources*, 195 (2010) 3680.
16. F. Lu, Y. Zhou, J. Liu and Y. Pan, *Electrochim. Acta*, 56 (2011) 8833.
17. C. M. Ban, W. J. Yin, H. W. Tang, S. H. Wei, Y. F. Yan and A. C. Dillon, *Adv. Energy Mater.*, 2 (2012) 1028.
18. S. Kim, V. Mathew, J. Kang,J. Gim, J. Song, J. Jo, and J. Kim, *Ceram. Int.*, 42 (2016) 7230.
19. A. Bünting, S. Uhlenbruck, and R. Vaßen, *J. Power Sources*, 281 (2015) 326.
20. Z. H. Wang, Q. Q. Pang, K. J. Deng, L. X. Yuan, F. Huang, Y. L. Peng and Y. H. Huang, *Electrochim. Acta*, 78 (2012) 576.
21. Z. J. Liu, X. J. Huang and D. S. Wang, *Solid State Commun.*, 147 (2008) 505.
22. S. H. Wu, M. Q. Chen, C. J. Chien and Y. P. Fu, *J. Power Sources*, 189 (2009) 440.
23. C. L. Fan, C. R. Lin, and X. Zhang, *New J. Chem.*, 38 (2014) 795.
24. G. G. Xu, K. H. Zhong, J. M. Zhang and Z. G. Huang, *Solid State Ion.*, 281 (2015) 1.
25. R. D. Shannon, *Acta. Cryst.*, 32 (1976) 751.
26. C. H. Zhang, Y. Z. Liang, L. Yao and Y. P. Qiu, *Solid State Ion.*, 267 (2014) 74.
27. C. L. Fan, S. C. Han, L. F. Li, Y. M. Bai, K. H. Zhang, J. Chen and X. Zhang, *J. Alloy Compd.*, 576 (2013) 18.
28. L. Li, X. Li, Z. Wang, L. Wu, J. Zheng and H. Guo, *J. Phys. Chem. Solids*, 70 (2009) 238.
29. G. X. Wang, S. Bewlay, S. A. Needham, H. K. Liu, R. S. Liu, V. A. Drozd, J. F. Lee, and J. M. Chen, *J. Electrochem. Soc.*, 153 (2006) A25.
30. F. H. Lu and H. Y. Chen, *Thin Solid Films*, 355 (1999) 374.
31. Y. P. Xu and J. Mao, *Ionics*, 21 (2015) 3159.
32. N. Mascaraque, J. L. G. Fierro, A. Durán and F. Muñoz, *Solid State Ion.*, 233 (2013) 73.
33. A. C. Kozen, A. J. Pearse, C. F. Lin, M. Noked and G. W. Rubloff, *Chem. Mater.*, 27 (2015) 5324.
34. K.F. Chiu, S. H. Su, H. J. Leu, and W. C. Huang, *Thin Solid Films*, 596 (2015) 34.
35. M. D. Levi and D. Aurbach, *J. Phys. Chem. B*, 101 (1997) 4630.